Electromechanical Model of a Conducting Polymer Transducer, Application to a Soft Gripper

Chia-Ju Peng, Olivier Ameline, Frédéric Braz Ribeiro, Cedric Plesse, Sinan Haliyo, Shih-Jui Chen, Luc Chassagne, Barthélemy Cagneau

IEEE Access
Multidisciplinary | Rapid Review | Open Access Journal

Received August 9, 2019, accepted August 29, 2019, date of publication September 18, 2019, date of current version November 5, 2019.

Digital Object Identifier 10.1109/ACCESS.2019.2942159

Electromechanical Model of a Conducting Polymer Transducer, Application to a Soft Gripper

CHIA-JU PENG[1,4], OLIVIER AMELINE[2], FRÉDÉRIC BRAZ RIBEIRO[3], CÉDRIC PLESSE[3], SINAN HALIYO[2], SHIH-JUI CHEN[4], LUC CHASSAGNE[1], AND BARTHÉLEMY CAGNEAU[1]

[1]UVSQ/LISV, Université de Versailles, 78140 Vélizy, France
[2]CNRS, Institut des Systèmes Intelligents et de Robotique, ISIR, Sorbonne Université, F-75005 Paris, France
[3]LPPI/I-MAT, University of Cergy-Pontoise, 95000 Cergy, France
[4]Department of Mechanical Engineering, National Central University, Taoyuan 320, Taiwan

Corresponding author: Barthélemy Cagneau (barthelemy.cagneau@uvsq.fr)

This work was supported in part by the French National Research Agency (ANR) and in part by the project MicroTIP.

ABSTRACT Conducting interpenetrating polymer networks (*C-IPN*) are a promising solution for the design of sensing and actuating parts at macro- or microscale. This class of polymers can be used in open-air, allowing for large displacements under low voltages with a reversible process. In this work, we are mainly interested in the electromechanical characterization of the material because of its particular behavior. Two working modes, namely actuation and sensing, are identified through modeling and experimental validations. The relationship between the output forces, the tip displacements and the driving voltages was highlighted with an experimental setup while actuating. On the other hand, the linear range and the sensitivity have been empirically modeled in sensing mode. We also demonstrate that this material is suitable to build a gripper for small objects. A sphere was lifted by the gripper, and the grasping force was successfully monitored by the sensing finger. This is a promising first step towards more complex 3D structures.

INDEX TERMS Soft robotics, end effectors, chemical sensors.

I. INTRODUCTION

Recent developments in the field of soft robotics are closely related to the improvement of materials required for the applications. In robotics, the need for soft actuators and soft sensors keeps increasing. However, the reason might be very different depending on the subfield: safety issues and environment awareness for humanoids [1], [2], integration constraints [3] in the fluidic environment, lack of specific tools [4] and fragile environment [5] in microrobotics. This paper focuses on a soft gripper made of a specific material which has been described in previous work [6] and [7]. Regarding the challenges in soft robotics, an ideal gripper could be basically presented as a mechanical structure suitable to grasp an object, in a compliant way, while monitoring the interaction forces. However, several steps are required to fulfill these requirements.

The first challenge is the design or the fabrication of the mechanical structure of the gripper. Because of the recent progress in technology, several solutions are based on 3D printing as in [8]. Moreover, 3D printing is not limited to classical ABS material. For example, in [9], the fingers are composed of two smart materials (shape memory polymer and conductive thermoplastic polyurethane) which are deposited on a substrate by a 3D printer. In [10], an electrothermal micro-gripper is composed of silver-nickel composite ink. In [11], compliant fingers are proposed to grasp soft objects. The final structure is made of different parts obtained with 3D printing methods. Besides 3D printing, more conventional techniques like photolithography are used to design soft grippers [12] made with Ionic Polymer Metal Composite (IPMC) [13].

The second challenge is to actuate the fingers. The solutions really depend on the task to perform. The range of the force produced as well as the power input are two key parameters to consider. In [14], the actuation is made with a high voltage ($\approx 3kV$) to generate electrostatic forces. In [15], because of the variable stiffness, it is possible to drive the foldable structure with respect to this parameter. As a consequence, the contact with the object may be chosen between

The associate editor coordinating the review of this manuscript and approving it for publication was Kai Li.

stiff and soft modes. Several grippers such as [16] or [17] are based on pneumatic actuators. The inflated volume may be in contact with the object or used to move a part of the structure towards the object. Shape Memory Alloys (SMA) are also good candidates for the design of micro-grippers [18], [19]. In this paper, we will use a subclass of Electroactive Polymers (EAP) to perform a grasping experiment. Because of the large deformation that they produce, EAP may be suitable for the design of grippers [20]. As explained in previous work [7], EAP are actuated with a low-voltage ($< 3\ V$) in open-air environment.

The third challenge to design soft grippers is the need for a feedback information. In several papers, like in [19] or [21], visual tracking is performed to compute the force applied by the finger on the object or to monitor its position. Another solution is to include strain sensors in the structure [22], [23]. The aim is indeed to add a sensor which is compatible with softness requirements. In [24], a resistive flex sensor is included into each finger so that the gripper is suitable for haptic identification. However, as stated in [25], the process of fabrication is often very constrained when the sensor is seen as an additional layer of the gripper. The EAP that we have fabricated for this work are called Conducting Interpenetrating Polymer Networks (C-IPNs). The functions to sense and actuate are achieved within the same material and allow for the design of a soft gripper.

In this paper, we focus on the electromechanical characterization and the experimental validations to evaluate the capability of C-IPNs as sensors or actuators, revealing the possibility to propose a gripper based on C-IPN material. Its chemical composition is briefly recalled in section II and more details on the full process are available in [26]. In the same section, the experimental setup is described as well as the steps required to implement the grasping task. In section III, the electrical and mechanical models of C-IPN are fully presented to further characterize the behaviors based on previous work [7]. The C-IPN is used as a cantilever to establish a relationship between the force and the deformation with respect to the driving voltage. We also demonstrate that the bending state of the cantilever is monitored while using an empirical model based on the output voltage.

A simple gripper is presented in section IV. We present the first results obtained to grasp a small object ($5.5mm$, $95mg$) with a 2-fingers configuration (one active and one passive). A linear model is presented to estimate the grasping force based on the output of the sensing finger. The models derived in previous sections are also useful to compute and track this force in real time. Finally, achievements and future improvements are discussed in section V.

II. SOFT MATERIAL FOR DUAL FUNCTIONALITIES

A. PHYSICO-CHEMICAL MATERIAL BACKGROUND ON C-IPN

C-IPN material displaying a trilayer structure (see figure 1) is based on a central membrane sandwiched by two layers of poly(3,4-ethylenedioxythiophene)(PEDOT).

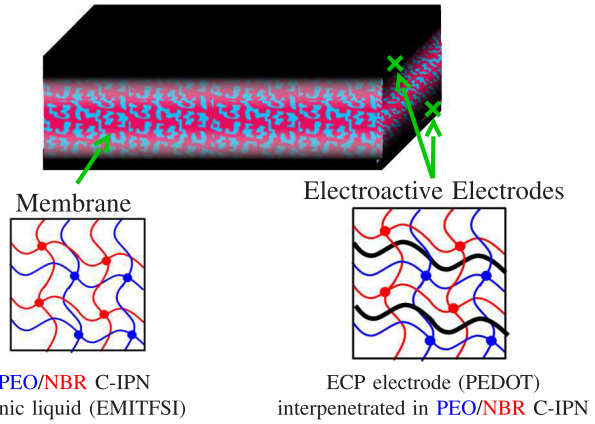

FIGURE 1. Schematic representation of the structure and composition of conducting C-IPN used as actuators or/and as sensors.

The central membrane acts as the ion reservoir membrane providing ions required for operating the device. This membrane is synthesized with an Interpenetrating Polymer Network (IPN) architecture which allows combining a poly(ethylene oxide) network insuring ionic conductivity in the presence of salt and a Nitrile Butadiene Rubber (NBR) network insuring the mechanical robustness of the final device. The ionic conducting membranes (PEO/NBR) is subsequently swollen in 3,4-ethylenedioxythiophene (EDOT), the monomer of the conducting polymer, and immersed into chemical oxidant solution(Aqueous FeCl3). This specific route allows the polymerization of EDOT into poly(3,4-ethylenedioxythiophene) (PEDOT) within the PEO/NBR membranes with a concentration gradient decreasing from the surface to the center of the resulting C-IPN, as depicted in figure 1. Once the C-IPN material is synthesized, the sample is then swollen with an electrolyte to obtain the final actuator/sensor device. The chosen electrolyte is the ionic liquid 1-ethyl-3-methylimidazolium bis(trifluoromethylsulfonyl)imide (EMITFSI) due to its high ionic conductivity and non-volatility [26].

B. CASE STUDY AND REQUIREMENTS

In figure 2, we present the different blocks which are necessary to characterize and drive the gripper. To demonstrate its feasibility, we chose to use one active finger (to actuate) and a passive one (to sense). The material used has been presented in section II-A.

The active polymer is driven with a low voltage, typically under $3\ V$. Its bending curvature depends on the sign of the potential difference. When the contact occurs between the object and the passive polymer, a potential difference is measured at the output (a few hundred of microvolts) and is amplified before being processed.

However, a relationship between the voltages and the external forces must be derived in order to control and to monitor the force during the experiment. For this purpose, a camera records the displacement of the active polymer and the

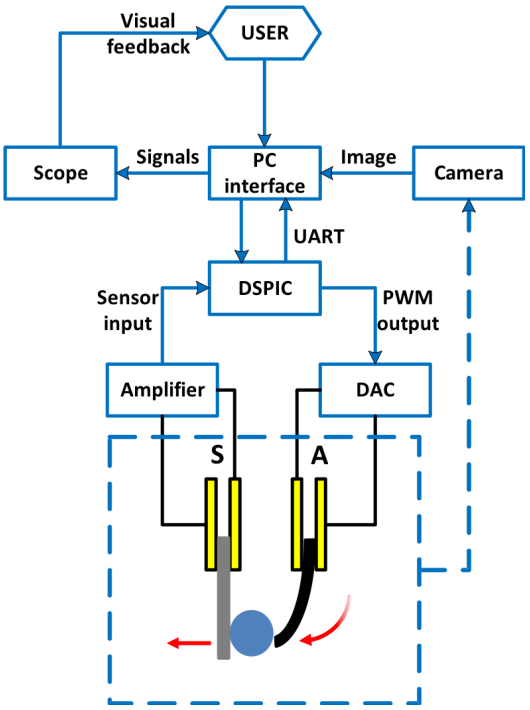

FIGURE 2. A gripper with one active and one passive finger. The block diagram illustrates the requirements to drive and process the signals.

passive polymer. The deformation and the curvature of the C-IPN are considerably large. This is challenging to measure distances with systems like laser. To measure the deformation and related forces of C-IPN with a large curvature, an image processing method is used and analyzes the lateral-view of the C-IPN recorded by the camera. Images are processed with a Sobel operator for edge detection. Since the lights, shadows, or any effects from the background influence the recorded image and cause imperfect detected edges, fragmented edge data are connected based on the algorithms of morphology. Applying the image processing procedure to the whole video, the shape of the C-IPN in each frame is obtained. Thus, the deformation of C-IPN cantilever can be tracked. The last tip displacement is used as the input of the mechanical model proposed in section III. On the other hand, the behavior of the passive polymer should be first identified based on its electrical response.

III. CHARACTERIZATION OF C-IPN TRANSDUCERS

A. ELECTRICAL RESPONSE

To characterize the electrical response of C-IPN, a hypothesis of equivalent circuits as an actuator and a sensor is presented in figure 3. The conducting polymer is modeled as a resistor serried with a parallel RC circuit based on the simplified Randles model [27], [28]. C_p represents a pseudocapacitance to store the electrochemical energy resulting from ions transport in the electrolyte [6]. The resistor R_p shows the possible current leakage when ions migrate. R_e represents the impedance between the polymer layers and electrodes.

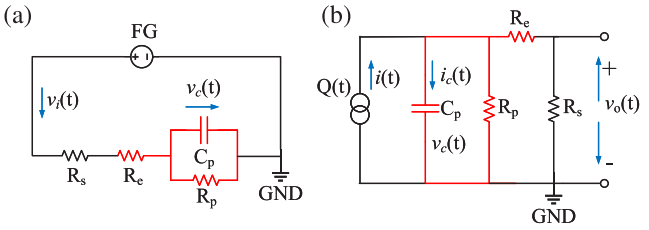

FIGURE 3. The equivalent circuits of a C-IPN marked in red as (a) an actuator and (b) a sensor. C_p: the pseudocapacitance to store the electrochemical energy, R_p: the resistance for possible current leakage, R_e: the serried resistance of the polymer layers and electrodes, R_s: the internal resistance of the apparatus for measurement, GND: the reference ground, $v_i(t)$: the input voltage to drive the actuator, $v_o(t)$: the output voltage of the sensor. The charge induced by the strain performs as a limited charge source $Q(t)$.

A resistor R_s is included to model the internal resistance of the apparatus for measuring the potential difference. For ease of control, the equivalent circuit we use is simplified through its mathematical form compared to the complex model that renders the physical structure. When C-IPN is driven, as shown in figure 3(a), the electron makes cathode of PEDOT reduced, and the anode of PEDOT oxidized. Since the mobility of cations and anions are different within the polyelectrolyte, the movable cation particles (EMI+) flow to the cathode to achieve electrical balance, while C_p is charged to model the redox reaction. The migration of ions generates mechanical work for actuation. On the other hand, when mechanical stimuli are applied to a C-IPN as shown in figure 3(b), the bending of the polymer layers changes the spatial distribution of the movable ions. Partial cations are squeezed out from the compressing layer and accumulate in the elongating layer, resulting in charge unbalance. A potential difference is generated between the parallel PEDOT electrodes. The amount of ion migration is represented by a limited induced charge source Q.

The validation of C-IPN sensor measurements is not straightforward. The sensing behavior of C-IPN is similar to piezoelectric sensors. The output voltage decays with time because of the internal impedances due to both sensor and apparatus for measurement. Therefore, C-IPN sensors are limited when measuring static or very-low-frequency forces. As a consequence, this behavior is problematic to sense while grasping an object. Assuming that the charge transfer depends on steady-state voltage attenuation, it follows that the voltage attenuation from one electrode to the other is equal to the loss of charge. When a C-IPN is bent under a static constraint, the induced charge Q is stored in C_p and is no longer generated if no leakage occurs. Let suppose that the output voltage remains constant during the static deformation. While the current flows out and the potential difference decays, a compensation method for the output voltage of C-IPN sensors can be used that [29]:

$$\begin{cases} v_{ss}(t) = v_o(t) + v_{comp}(t) \\ v_{comp}(t) = \dfrac{R_p + R_s + R_e}{CR_pR_s} \displaystyle\int v_o(t)dt - \frac{1}{C} \int i_b(t)dt \end{cases} \quad (1)$$

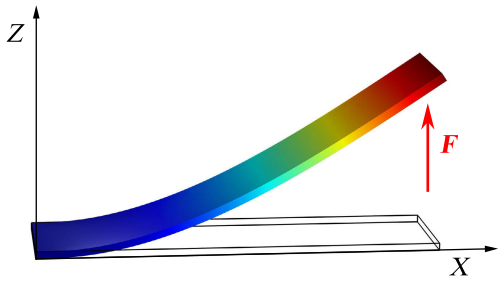

FIGURE 4. Mechanical model of the C-IPN cantilever. As an actuator, the generated force F deforms the polymer itself and can be used for grasping. On the other hand, as a sensor, the external force F applied on the tip can be approximately obtained with corresponding deformation.

where $v_{ss}(t)$ is the steady-state output of the bent C-IPN after the compensation, i_b is the bias current of the amplifier or devices that should be removed. With Equation 1, the compensating voltage $v_{comp}(t)$ can be estimated over time and balance the leakage during the quasi-static deformation.

B. MECHANICAL RESPONSE

A mechanical model is used to estimate the force generated by the active finger of the gripper. The polymer is considered as an elastic rod without extension or shearing. As represented in figure 4, the action of the flowing current is approximated by a unique vertical force **F** applied at the free end of the rod. It is considered predominant over gravity, which can be double-checked based on the experimental validations.

Furthermore, the material is assumed to be isotropic and uniform with linear elastic constitutive relations. The actuator is considered straight in its unstressed state. Under a quasi-static approximation, inertia effects are neglected and only equilibrium configurations are computed.

The large static deformation of such a rod, called an Euler elastica, has been studied for centuries [30]. The mechanical equilibrium results in ordinary differential equations whose solutions can be expressed as analytically in terms of Jacobi elliptic functions. These solutions are classified into two categories : the inflexional and the non-inflexional Euler elastica. As no moment is applied at the free end of the rod, this end is a point of inflexion of the shape. As a consequence, the actuator is represented by the inflexional case.

Let E be the Young modulus of the polymer and I the moment of inertia of sections perpendicularly to the plane of the rod. It is useful to choose $\sqrt{EI/F}$ as the unit of length. With this setting, the shape of the actuator is described by the evolution of the dimensionless coordinates (x, z) as functions of a dimensionless abscissa s. In a judicious reference frame for which the axis z is in the same direction as the applied force, this shape is parametrized by a quantity $m \in [0, 1]$ called the modulus [30]:

$$\begin{cases} x(s,m) = 2\sqrt{m}\,\mathrm{cn}(s,m) \\ z(s,m) = s - 2E\,(\mathrm{am}(s,m),m) \end{cases} \tag{2}$$

where $\mathrm{cn}(\cdot, m)$ is the cosine function of Jacobi and $E(\cdot, m)$ the elliptic integral of the second kind.

In system 2, the bounds of abscissa s are determined by writing the boundary conditions of the experimental shape. As the tangent at the clamped end of the rod is perpendicular to the force applied at the free end, the shape of the actuator begins at an abscissa s_i where the derivative of coordinate z is null. In [31], s_i is given by:

$$s_i = \mathrm{cn}^{-1}\left(\sqrt{\frac{-1+2m}{2m}}, m\right) \tag{3}$$

As mentioned above, the free end of the actuator is a point of inflexion. This implies that the shape terminates at the abscissa s_f defined as

$$s_f = K(m) \tag{4}$$

where $K(m)$ is the complete elliptic integral of the first kind. As a result, the rod has a dimensionless length

$$l = s_f - s_i \tag{5}$$

Noting L the dimensioned length of the polymer and (X, Z) the dimensioned coordinates, the shape is given by

$$\begin{cases} X(S,m) = -\dfrac{L}{l}\left[x\left(\dfrac{l}{L}S + s_i\right) - x(s_i)\right] \\ Z(S,m) = \dfrac{L}{l}\left[z\left(\dfrac{l}{L}S + s_i\right) - z(s_i)\right] \end{cases} \tag{6}$$

where $S \in [0, L]$ denotes the dimensioned curvilinear abscissa.

System 6 is completely determined when the modulus m is known. Because s_i is a local extremum of coordinate z, m is confined within [0.5, 1] [31]. Its value is determined by a fit to the maximal deflection d_{max} of the rod, which is known experimentally and connected to m through

$$d_{max} = Z(L, m) \tag{7}$$

Inversion of equation 7 is straightforward because $Z(L, m)$ evolves linearly with m on the range of measured deflections.

Once the value of m is computed, the force F is obtained by writing that the unit of length $\sqrt{EI/F}$ is also the ratio L/l, thus

$$F = EI \cdot \left(\frac{l}{L}\right)^2 \tag{8}$$

Expression 8 is an estimation of the force applied by the actuator.

C. ACTUATOR BEHAVIORS

The objective is now to validate the mechanical model for C-IPN actuators. Hereafter, an actuating cantilever made of C-IPN is used. Its Young modulus is $E = 150\ MPa$ for a width of 4 mm and a thickness of $250\mu m$. The length L is 24 mm or 10 mm depending on the experiments.

In a first experiment, the actuator measures 24 mm and is actuated with an input voltage of 2.5 V. A camera tracks the displacement with respect to the time. The images are then processed to determine the shape of the polymer.

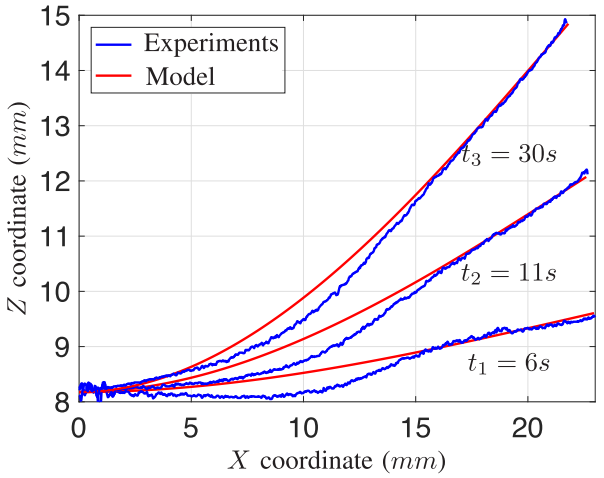

FIGURE 5. Experimental and modeled shapes of the polymer for different time values. The actuator is actuated at 2.5 *V*. Its length *L* is 24 *mm*.

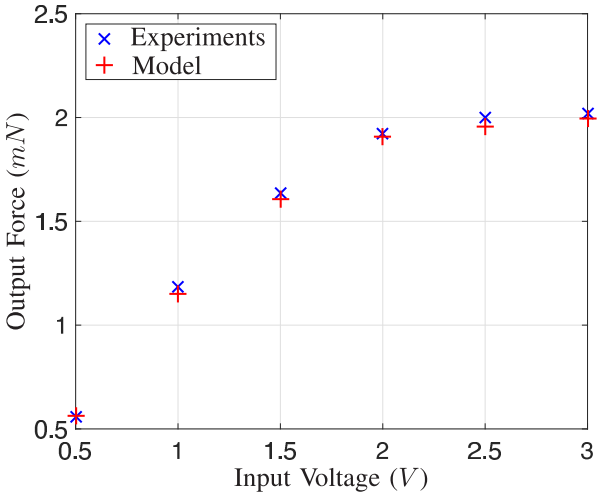

FIGURE 6. The estimated actuating forces with respect to different input voltages. The length *L* of the actuator is 10 *mm*.

Figure 5 represents the experimental and theoretical shapes at times $t_1 = 6\,s$, $t_2 = 11\,s$ and $t_3 = 30\,s$.

A good agreement is obtained between the model presented in equation 6 and experimental data, especially when the X coordinate is higher than 15 mm. One reason is that, because of the fabrication process at macro-scale, the polymer is not perfectly flat. This is pretty obvious when looking at the shapes for t_1 and t_2. However, in the scope of this paper, we are mainly interested in results close to the tip of the actuator. This part is indeed in contact with the object.

In a second experiment, the C-IPN actuator is in contact with a spring of a known stiffness $k = 8.0mN.mm^{-1}$. The deformation of the spring is tracked with image processing, and the force that the polymer applies to it is measured. For this experiment, the length of the polymer is $L = 10\ mm$. The input voltage is set to different values in the range of $[0.5\ V,\ 3.0\ V]$. For each value, equation 8 is used to compute the force. The comparison between experimental data and the model is presented in figure 6.

The maximum force generated with the polymer is around 2.0 mN. 95% of this value is reached when the input voltage is set to 2.5 V. There is no need to exceed this value as long as the force magnitude is concerned. A higher voltage will result in better dynamical performances but may decrease the life of the material.

In figure 7, the applied force measured with the spring is plotted against the maximal deflection (so-called free tip displacement), which is measured when C-IPN bends without any constraint at the tip. The relation between the force and the free tip displacement can be fitted with a linear approximation, and the rate is 0.81 $mN.mm^{-1}$. Regarding the final experiment of grasping presented in section IV, the mathematical model seems suitable to anticipate for the force applied by the polymer on an object such that:

$$F = \beta \cdot d \tag{9}$$

where the ratio β is 0.81 $mN.mm^{-1}$.

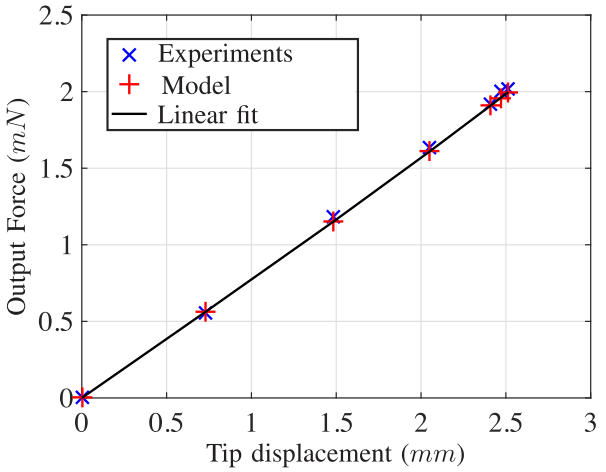

FIGURE 7. Maximum values of the actuating forces with respect to the free tip displacements. The corresponding input voltages are the same as in figure 6.

D. SENSOR BEHAVIORS

The experimental setup used to monitor the output voltage in sensing mode is shown in figure 8. A C-IPN sensor is fixed vertically above a slider. A linear motor is actuated with controlled velocities and accelerations to produce a mechanical disturbance to the C-IPN. The output voltage of the C-IPN sensor is amplified with a gain of 10000 for measurement. It is then divided by the same value to obtain the original value while postprocessing data.

To investigate the stability and repeatability of the C-IPN sensor, the output voltage produced by the periodic mechanical disturbance is studied. The linear motor moved back and forth to push the tip of the C-IPN at a constant velocity. The bending frequency is set to 0.5 Hz. Figure 9 presents the sensing outputs with the displacement of 1.0 mm and 3.0 mm for demonstration. The first mechanical stimulus of the periodic disturbance induces the highest output marked with circles and noted as V_f. The trend of the periodic output

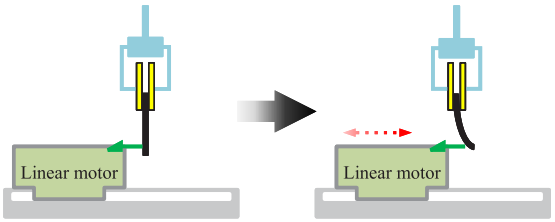

FIGURE 8. A C-IPN sensor was fixed vertically above a slider. The linear motor moved back and forth to push the tip of the C-IPN at a constant velocity.

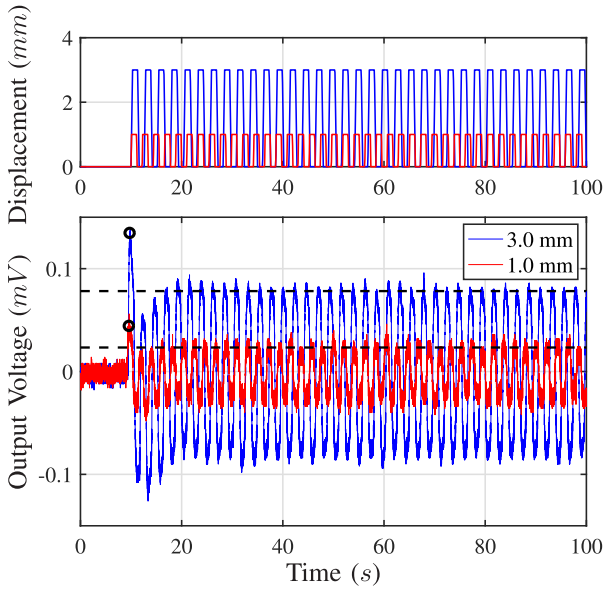

FIGURE 9. The output voltages of the C-IPN sensor (bottom) generated by different periodic mechanical disturbances (top). The dash lines represent the mean value of the maximal output voltages in the steady state (V_a) when the displacement is 1.0 *mm* or 3.0 *mm*. The circles mark the output voltage induced by the first disturbance (V_f).

voltages decreases first and then raises until reaching a steady state. A possible explanation is that the initial output voltage varies for each stimulus. Therefore, it takes time to recover from the negative potential of the previous one. Dash lines denote the mean value of the maximum output voltage (noted V_a) over several cycles.

Figure 10 compares the output voltages of the C-IPN sensor induced by the first disturbances (V_f) and the average outputs induced by the periodic disturbances in the steady state (V_a) ranging from 0.5 *mm* to 4.0 *mm*. The stability of the sensor highly depends on the consistency in the linear variation of the output; hence, the linear behaviors of V_f and V_a are desired which might be used for electromechanical modeling. Considering the good linearity and the sufficient manipulating range, the linear range of the C-IPN sensor was selected as [0 *mm*, 3 *mm*]. Non-linearity is often quantified in terms of the maximum deviations from the linear fitting and is expressed as a percentage of the output span. The sensitivity of V_f and V_a in this experiment were 0.048 $V.m^{-1}$ and 0.029 $V.m^{-1}$ based on the slope of the straight line as shown in figure 10.

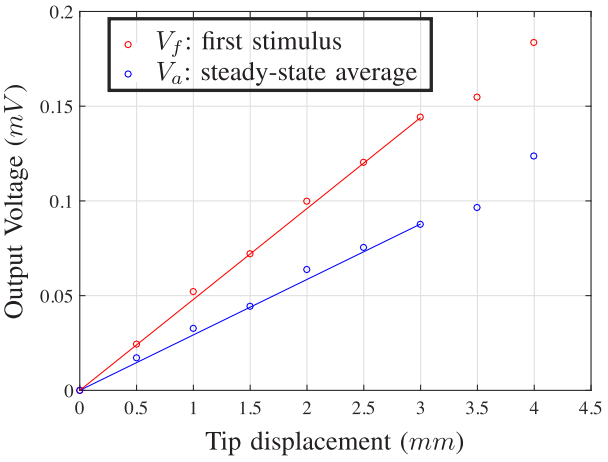

FIGURE 10. The output voltages of the C-IPN sensor with respect to the tip displacements generated by the linear motor. The slope of the linear fittings of V_f and V_a: 0.048 $V.m^{-1}$ and 0.029 $V.m^{-1}$.

Besides, it should be noted that the rising speed of the voltage and the maximum voltage are influenced by the speed of the deformation [7]. Despite the fact that a constant displacement is applied, V_f and V_a may vary if using a different bending frequency. Therefore, the red and blue straight lines respectively represent the linear responses of V_f and V_a in the defined range at this frequency.

IV. A SOFT GRIPPER MADE OF C-IPN

A. EXPERIMENTAL SETUP

The experiment that we conduct is described in figure 11(a). As explained in section II-B, the gripper system is composed of two C-IPN with dimensions of 10 *mm* × 4 *mm* × 0.25 *mm*. The first one, on the right side, is the active part. The second one, on the left side, is the sensing part. A small object, with a diameter of 5.5 *mm* and a mass of 95 *mg*, is placed between the two polymers. The gripping forces between the fingers and the object are noted $\mathbf{F_1}$ and $\mathbf{F_2}$.

Figure 11(b) ∼ 11(e) provide the technical aspects of the experimental setup. The user interface, programmed in C language, is presented in figure 11(b). It communicates with a dsPIC module (dspic33ep512mu810, *Microchip*) shown in figure 11(c) and in charge of data processing between the peripherals. While actuating, the dsPIC controls an electronic board shown in figure 11(d). The electronic board is based on a DAC8830 (*Texas Instruments*) and designed to generate input signal to drive the active finger. The gripping force can be modified with respect to the input voltage in the range of $\pm 2.5V$. While sensing, the potential difference of the passive finger is amplified by an amplifier circuit with a gain of 1210 before measurement. It is shown in figure 11(e).

In figure 12, several steps are completed during the grasping experiment:

(a) The gripper is opened and the input voltage of the active finger is switched to 2.5 V. According to figure 6,

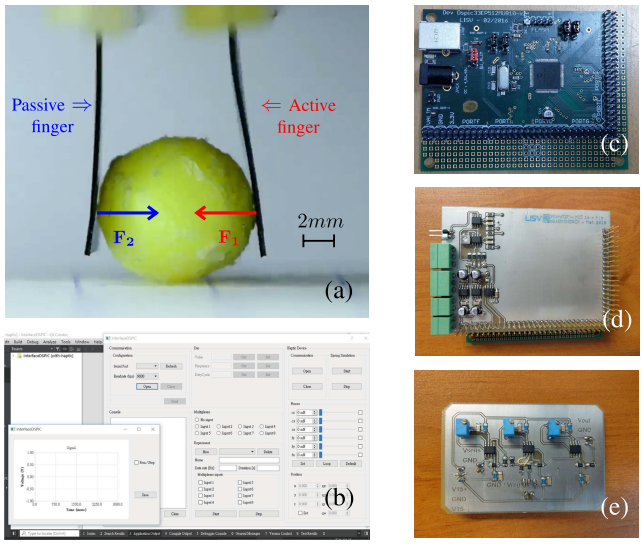

FIGURE 11. a) The two fingers are made of C-IPN. The object is a plastic bead (mass of 95 *mg*). b) The user interface with the scope. c) The dsPIC module for signal processing and control. d) The electronic board for driving the active finger. e) The amplifier circuit for the passive finger.

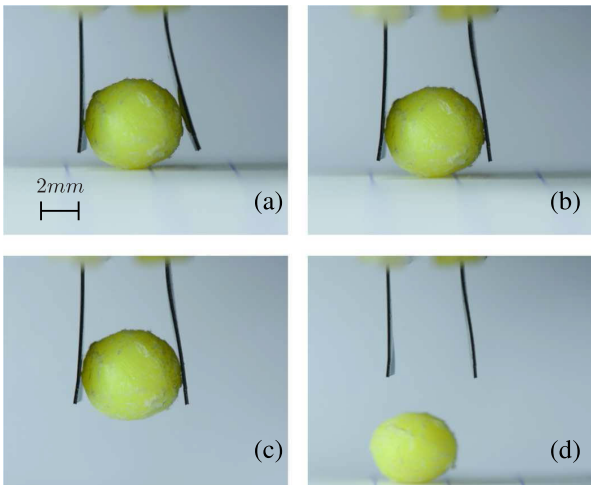

FIGURE 12. The grasping task is realized. The input voltage of the active finger is set to ±2.5 *V* to open or close the gripper.

the applied force on the object is $\|\mathbf{F_1}\| \approx 2.0\ mN$.

(b) The gripper is closing and the camera tracks the displacement of the tip. The difference of potential between the two electrodes of the passive finger is measured. We can expect $\|\mathbf{F_1}\| \neq \|\mathbf{F_2}\|$ because of the friction forces.

(c) The gripper is now fully closed and the object is lifted up. The active finger, as well as the passive one, apply a constant force on the object so that $\|\mathbf{F_1}\| = \|\mathbf{F_2}\|$.

(d) The input voltage of the active finger is switched to $-2.5\ V$ and the gripper is opening. As a consequence, the object is released and dropped.

B. EXPERIMENTAL RESULTS

In figure 13, the camera is used with image processing to measure the displacement of the active finger and the passive

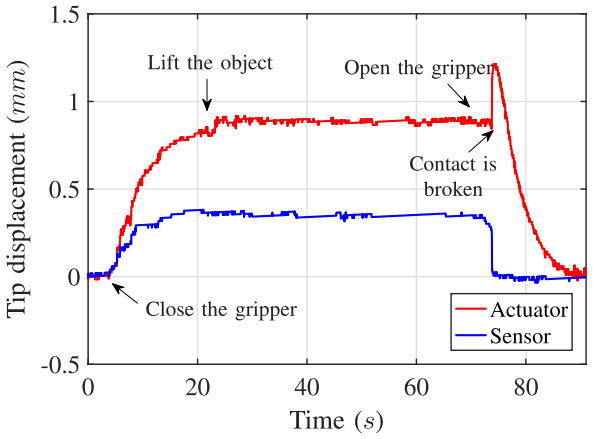

FIGURE 13. Displacement of the tip of the active finger. A peak occurs when the object is dropped.

finger. The positions correspond to the tip of the polymers. The results are consistent with the experiment described in figure 12. The tip of the active finger is first getting closer to the object. Next, the displacement reaches a maximum value around 0.9 *mm*. The active finger applies now a constant force on the object that corresponds to a specific position, when the passive finger is pushed by the object with a displacement of 0.35 *mm*. The object is then dropped, and a peak appears on the figure at a time $t \approx 72\ s$. When the gripper is fully opened, the tip returns to its initial position.

The measured voltage on the passive finger is shown in figure 14, which is divided by gain of the amplifier to retrieve the original value. This figure is closely linked to figure 13. When the contact is established, the measured voltage on the passive finger linearly increases. The constraint is then maintained with a constant force, and the output voltage is slowly decreasing. The time constant for the discharge is approximately 20 *s*. When the contact is broken, the measured voltage on the passive finger is then dropping quickly and reaches a minimum value of $-0.06\ V$. However, the sensing output of the passive finger is susceptible to external interference such as the driving device of the active finger or the environmental noise.

C. SENSING MEASUREMENTS AND VALIDATIONS

The relation between the output voltage and the applied force of the passive finger should be identified. One possible experimental setup could be using a tiny and precise force generator or actuator to bend a passive C-IPN with micronewtons. Another solution is using the active polymer to bend the passive one together. Hereafter, two C-IPN (one active and one passive) are attached together without any electrical conduction to form an integrated finger. When the active part is actuating, the passive part is bending too and outputs the sensing voltage. Figure 15 compares the sensing output of this setup with the gripping system. The tip displacement d and the applied force F of the passive part of integrated finger

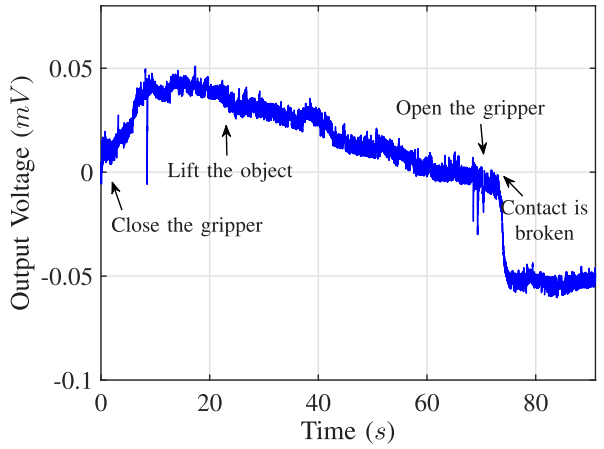

FIGURE 14. Measured potential voltage between the two electrodes of the passive finger.

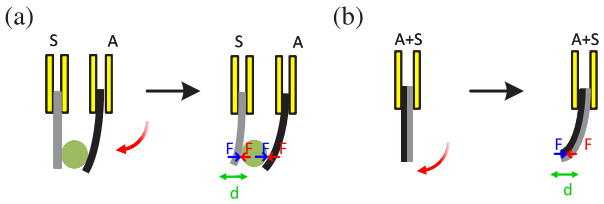

FIGURE 15. (a) The active finger pushes the object as well as the sensing finger. (b) The active and sensing part of integrated finger bend together. The tip displacement d and the applied force F of the sensing polymer are assumed to be equal in these two setups.

(see Figure 15(b)) and the passive finger of the soft gripper (see Figure 15(a)) are assumed to be equal. Thus we may use this integrated finger to simulate the grasping force of the gripper.

The active part of polymer is driven and bends. Meanwhile, the passive part of the polymer is bent together with the active one and produces the potential difference. The output voltage of the passive part is measured. During the experiment, the active part is actuated with a constant voltage. The displacement reaches its maximum value (bending state) and is kept constant for a while (holding state). The input voltage of the active part is then set to 0 V and the whole C-IPN starts to relax. Figure 16 shows the experimental results of the sensing output with respect to different driving voltages of the active part. While measuring the tip displacement, the output voltage can be linked to the input force of the active polymer based on the same displacement of the tip.

In figure 16, the active part is driven from 0.5 V to 2.0 V. Due to the constraint of the passive finger, the displacement and the corresponding output voltage are smaller, and the electrical interferences due to the environment are evident. While bending, the original output voltage (blue) rises up until reaching its maximal value. The slope varies because of the actuating speed with respect to the driving input. As previously explained, the voltage gradually decays due to the leakage. The method mentioned above is applied to compensate for the leaked charge using equation 1. After

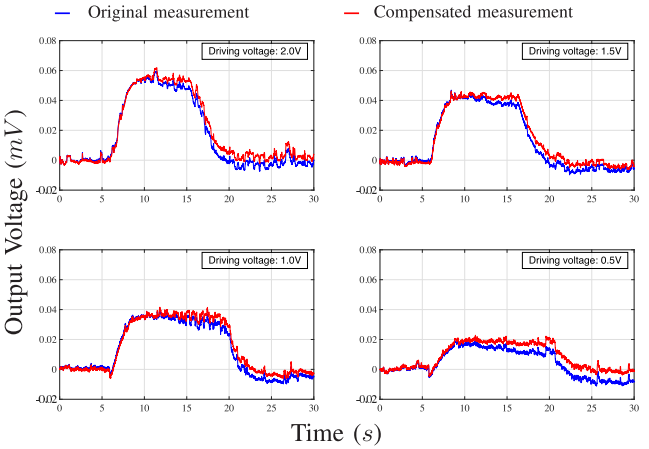

FIGURE 16. The comparison of sensing outputs of the integrated C-IPN before (blue) and after (red) the compensation. The driving voltage of the active part: (a) 2.0V, (b) 1.5V, (c) 1.0V, (d) 0.5V.

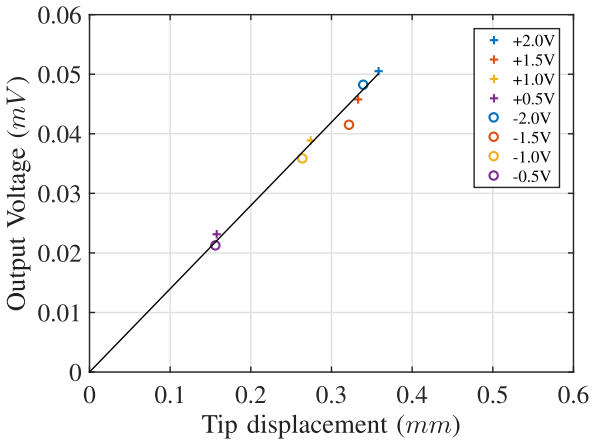

FIGURE 17. The output voltage of the passive C-IPN against the tip displacement generated from the active C-IPN. The sensitivity of the passive C-IPN is 0.1398 V/m.

compensation, the output (red) remains constant when the polymer reaches its maximal deformation.

The transient behavior of the sensor is presented in figure 17. It shows the output voltage of the passive part against the tip displacement. The results for negative driving inputs (from -0.5 V to -2.0 V) are plotted to check for symmetric displacements of the polymer. Moreover, the sensing output is supposed to be proportional to the displacement within the dynamic range. In this study, we build the relation of sensor output so that:

$$v = \alpha \cdot d \tag{10}$$

where $\alpha = 0.1398\ mV.mm^{-1}$ is a constant ratio, d is the tip displacement of the C-IPN sensor.

With these results, the integrated C-IPN cantilever can monitor the tip displacement or even the generated force with the measurement of sensing output, which is helpful to monitor the output of the gripping fingers. Moreover, we combine equation 9 and equation 10 to link the generated force of active finger and the sensing output of the passive

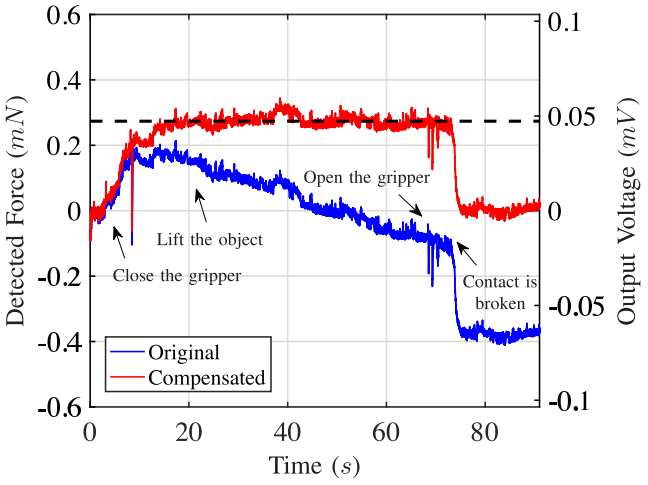

FIGURE 18. Measured potential voltage between the two electrodes of the passive finger before and after the compensation. The mean of voltage during the grasping is 0.0473 *mV*, pointing the detected grasping force of 0.2741 *mN* with the sensitivity of 5.7939 *N*/*V*.

finger through the tip displacement that:

$$F(t) = \gamma \cdot v(t) \tag{11}$$

where $\gamma = \frac{\beta}{\alpha}$ is a constant ratio, $\gamma = 5.7939\ mN.mV^{-1}$.

Figure 18 compares the sensing output (see figure 14) before and after the compensation of the discharge with equation 1. The mean value of the voltage during the grasping is $0.0473mV$ for a displacement of $0.35mm$. There is an agreement with the figure 17 that the value approaches $0.0489mV$ according to equation 10. Equation 11 estimates the grasping force of the gripper based on the sensing output of the passive finger. In the holding state, as shown in figure 12(c), the gripper grasps the object, and two fingers apply a constant force on the object $\|\mathbf{F_1}\| = \|\mathbf{F_2}\| \approx 0.2741\ mN$. As a consequence, the gripping force is successfully monitored with the sensing output as shown in figure 18.

V. CONCLUSION

In this paper, we have presented an original approach to describe the behaviors of a polymer transducer. For the first time, we were able to derive and use electromechanical models to propose a soft gripper and monitor the grasping force in real time. To realize this prototype, the linear dynamic range and the sensitivity of the C-IPN sensor were analyzed with mechanical and electrical responses. The C-IPN actuator provided a value of the force applied on an object with respect to the driving voltage. The relationship between the output force, the tip displacement and the driving voltage of the C-IPN actuator were highlighted with experiments. Moreover, a setup with a gripper composed of two fingers has been proposed. A small object was successfully lifted, and it was able to detect the time when the contact was broken during the release phase. The empirical models were useful to predict the output force generated by the C-IPN. The gripping force was monitored with the corresponding sensing output by the linear model of the C-IPN sensor.

Compared to other systems, C-IPNs are promising in soft robotics and micro-robotics as a solution for the design of soft structures that are capable to sense and actuate on the same material, for instance. Its design is compatible with usual techniques used for the fabrication of MEMS. However, the behavior of the C-IPN at microscale needs to be investigated to propose a similar gripper at this scale.

REFERENCES

[1] T. Someya, T. Sekitani, S. Iba, Y. Kato, H. Kawaguchi, and T. Sakurai, "A large-area, flexible pressure sensor matrix with organic field-effect transistors for artificial skin applications," *Proc. Nat. Acad. Sci. USA*, vol. 101, no. 27, pp. 9966–9970, 2004.

[2] B. C.-K. Tee, C. Wang, R. Allen, and Z. Bao, "An electrically and mechanically self-healing composite with pressure- and flexion-sensitive properties for electronic skin applications," *Nature Nanotechnol.*, vol. 7, pp. 825–832, Nov. 2012.

[3] Y. K. Lee and I. Shimoyama, "A multi-channel micro valve for micro pneumatic artificial muscle," in *Proc. IEEE Int. Conf. 15th IEEE Int. Conf. Micro Electro Mech. Syst.*, Jan. 2002, pp. 702–705.

[4] J. C. Breger, C. Yoon, R. Xiao, H. R. Kwag, M. O. Wang, J. P. Fisher, T. D. Nguyen, and D. H. Gracias, "Self-folding thermo-magnetically responsive soft microgrippers," *ACS Appl. Mater. Interfaces*, vol. 7, no. 5, pp. 3398–3405, Jan. 2015.

[5] K. Yoshida, N. Tsukamoto, J.-W. Kim, and S. Yokota, "A study on a soft microgripper using MEMS-based divided electrode type flexible electro-rheological valves," *Mechatronics*, vol. 29, pp. 103–109, Aug. 2015.

[6] C.-J. Peng, T. A. Nguyen, K. Rohtlaid, C. Plesse, S.-J. Chen, L. Chassagne, and B. Cagneau, "A versatile conducting interpenetrating polymer network for sensing and actuation," in *Proc. IEEE Int. Conf. Robot. Automat. (ICRA)*, May/Jun. 2017, pp. 4321–4325.

[7] T. A. Nguyen, C.-J. Peng, K. Rohtlaid, C. Plesse, T.-M. G. Nguyen, F. Vidal, S.-J. Chen, L. Chassagne, and B. Cagneau, "Conducting interpenetrating polymer network to sense and actuate: Measurements and modeling," *Sens. Actuators A, Phys.*, vol. 272, pp. 325–333, Apr. 2018.

[8] R. R. Ma, L. U. Odhner, and A. M. Dollar, "A modular, open-source 3D printed underactuated hand," in *Proc. IEEE Int. Conf. Robot. Automat.*, May 2013, pp. 2737–2743.

[9] Y. Yang and Y. Chen, "3D printing of smart materials for robotics with variable stiffness and position feedback," in *Proc. IEEE Int. Conf. Adv. Intell. Mechatronics (AIM)*, Jul. 2017, pp. 418–423.

[10] Y.-Y. Feng, S.-J. Chen, P.-H. Hsieh, and W.-T. Chu, "Fabrication of an electro-thermal micro-gripper with elliptical cross-sections using silver-nickel composite ink," *Sens. Actuators A, Phys.*, vol. 245, pp. 106–112, Jul. 2016.

[11] Z. Wang and S. Hirai, "A 3D printed soft gripper integrated with curvature sensor for studying soft grasping," in *Proc. IEEE/SICE Int. Symp. Syst. Integr. (SII)*, Dec. 2016, pp. 629–633.

[12] G.-H. Feng and S.-C. Yen, "Micromanipulation tool replaceable soft actuator with gripping force enhancing and output motion converting mechanisms," in *Proc. 18th Int. Conf. Solid-State Sens., Actuators Microsyst. (TRANSDUCERS)*, Jun. 2015, pp. 1877–1880.

[13] O. U. Khan, W. A. Lughmani, A. Wakeel, and S. U. Rehman, "Finite element modeling of blocking force of ionic polymer metal composites (IPMC) in micro gripper," in *Proc. 13th Int. Conf. Emerg. Technol. (ICET)*, Dec. 2017, pp. 1–5.

[14] E. W. Schaler, D. Ruffatto, P. Glick, V. White, and A. Parness, "An electrostatic gripper for flexible objects," in *Proc. IEEE/RSJ Int. Conf. Intell. Robots Syst. (IROS)*, Sep. 2017, pp. 1172–1179.

[15] A. Firouzeh and J. Paik, "Grasp mode and compliance control of an underactuated origami gripper using adjustable stiffness joints," *IEEE/ASME Trans. Mechatronics*, vol. 22, no. 5, pp. 2165–2173, Oct. 2017.

[16] J.-Y. Nagase, S. Wakimoto, T. Satoh, N. Saga, and K. Suzumori, "Design of a variable-stiffness robotic hand using pneumatic soft rubber actuators," *Smart Mater. Struct.*, vol. 20, no. 10, Aug. 2011, Art. no. 105015.

[17] L. Hines, K. Petersen, and M. Sitti, "Asymmetric stable deformations in inflated dielectric elastomer actuators," in *Proc. IEEE Int. Conf. Robot. Automat. (ICRA)*, May/Jun. 2017, pp. 4326–4331.

[18] R. J. Chang and C. C. Shiu, "Vision-based control of SMA-actuated polymer microgripper with force sensing," in *Proc. IEEE Int. Conf. Mechatronics Automat.*, Aug. 2011, pp. 2095–2100.

[19] R.-J. Chang and C.-Y. Cheng, "Vision-based compliant-joint polymer force sensor integrated with microgripper for measuring gripping force," in *Proc. IEEE/ASME Int. Conf. Adv. Intell. Mechatronics*, Jul. 2009, pp. 18–23.
[20] G. Alici and N. N. Huynh, "A robotic gripper based on conducting polymer actuators," in *Proc. 9th IEEE Int. Workshop Adv. Motion Control*, Mar. 2006, pp. 472–477.
[21] S. Bhattacharya, B. Bepari, and S. Bhaumik, "Novel approach of IPMC actuated finger for micro-gripping," in *Proc. Int. Conf. Inform., Electron. Vis. (ICIEV)*, Jun. 2015, pp. 1–6.
[22] Y.-L. Park, K. Chau, R. J. Black, and M. R. Cutkosky, "Force sensing robot fingers using embedded fiber Bragg grating sensors and shape deposition manufacturing," in *Proc. IEEE Int. Conf. Robot. Automat.*, Apr. 2007, pp. 1510–1516.
[23] K. Elgeneidy, G. Neumann, M. Jackson, and N. Lohse, "Directly printable flexible strain sensors for bending and contact feedback of soft actuators," *Frontiers Robot. AI*, vol. 5, p. 2, Feb. 2018.
[24] B. S. Homberg, R. K. Katzschmann, M. R. Dogar, and D. Rus, "Haptic identification of objects using a modular soft robotic gripper," in *Proc. IEEE/RSJ Int. Conf. Intell. Robots Syst. (IROS)*, Sep./Oct. 2015, pp. 1698–1705.
[25] R. A. Bilodeau, E. L. White, and R. K. Kramer, "Monolithic fabrication of sensors and actuators in a soft robotic gripper," in *Proc. IEEE/RSJ Int. Conf. Intell. Robots Syst. (IROS)*, Sep./Oct. 2015, pp. 2324–2329.
[26] N. Festin, A. Maziz, C. Plesse, D. Teyssié, C. Chevrot, and F. Vidal, "Robust solid polymer electrolyte for conducting IPN actuators," *Smart Mater. Struct.*, vol. 22, no. 10, Sep. 2013, Art. no. 104005.
[27] Jo. D. Madden, P. G. Madden, and I. W. Hunter, "Conducting polymer actuators as engineering materials," *Proc. SPIE*, vol. 4695, pp. 176–191, Jul. 2002.
[28] J. F. Rubinson and Y. P. Kayinamura, "Charge transport in conducting polymers: Insights from impedance spectroscopy," *Chem. Soc. Rev.*, vol. 38, no. 12, pp. 3339–3347, 2009.
[29] C.-J. Peng, F. Ribeiro, C. Plesse, S.-J. Chen, L. Chassagne, and B. Cagneau, "Electrical behavior of a self-sensing actuator made of electroactive polymers," in *Proc. 2nd IEEE Int. Conf. Soft Robot. (RoboSoft)*, Apr. 2019, pp. 212–216.
[30] A. E. H. Love, *A Treatise on the Mathematical Theory of Elasticity*. Cambridge, U.K.: Cambridge Univ. Press, 1893.
[31] O. Ameline, S. Haliyo, X. Huang, and J. A. H. Cognet, "Classifications of ideal 3D elastica shapes at equilibrium," *J. Math. Phys.*, vol. 58, no. 6, Jun. 2017, Art. no. 062902.

CHIA-JU PENG received the B.S. degree in agriculture (with a minor in bio-industrial mechatronics engineering) from National Taiwan University, Taipei, Taiwan, in 2012. He is currently pursuing the joint Ph.D. degree in mechanical engineering with National Central University, Taoyuan, Taiwan, and the Université de Versailles Saint-Quentin en Yvelines UVSQ/LISV, Vélizy, France. His research interests include biosignal processing, image processing, microelectromechanical systems, robotics, and transducers.

OLIVIER AMELINE received the Ph.D. degree from the Institute of Intelligent Systems and Robotics (ISIR), Sorbonne University, in 2018. His main research interest includes mathematics modeling of structures with applied mechanics.

FRÉDÉRIC BRAZ RIBEIRO received the master's degree in polymer chemistry from the University of Cergy-Pontoise, in 2016. He is currently pursuing the Ph.D. in Microsystem including Transducers based Interpenetrated Polymer networks (micro-TIP project) with the Laboratory of Physical-Chemistry of Polymers and Interfaces (LPPI), University of Cergy-Pontoise. The goal of his work is to develop fully-dried conducting-IPN microactuators by designing and synthesizing a new generation of ion reservoir membrane by using polymeric ionic liquids (PILs).

CÉDRIC PLESSE received the Ph.D. degree in macromolecular chemistry from the University of Cergy-Pontoise, in 2004, and the Habilitation (HDR) degree, in 2014. He was a Postdoctoral Researcher with the Mario Leclerc's Laboratory, University of Laval, Canada, from 2004 to 2006. He was then recruited as an Associate Professor with the Laboratory of Physicochemistry of Polymers and Interfaces (LPPI), University of Cergy-Pontoise, in 2006. His main research interests include the development of conducting polymer-based electrostimulable materials from the synthesis of highly conducting ionogels with interpenetrating polymer network architectures to electromechanical characterization of synthesized (macro or micro) actuators.

SINAN HALIYO is currently an Associate Professor with the Institute of Intelligent Systems and Robotics (ISIR), Sorbonne University, Paris, and has been active in robotics, since 1999. His current research interests include control and design issues, physical interactions and user interfaces for micro-scale applications in assembly, characterization, and user training. He also takes a particular interest in human–computer interaction issues in remote handling and teleoperation, especially with haptics and multimodal interfaces.

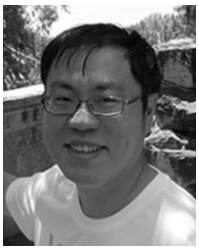

SHIH-JUI CHEN is currently an Associate Professor with National Central University, Taoyuan, Taiwan. His research interests include microelectromechanical systems, acoustic, and piezoelectric transducers.

LUC CHASSAGNE received the B.S. degree in electrical engineering from Supelec, France, in 1994, and the Ph.D. degree in optoelectronics from the University of Paris XI, Orsay, France, in 2000, for his work in the field of atomic frequency standard metrology. He is currently a Professor and the Director of the LISV Laboratory, University of Versailles. His research interests include nanometrology, sensors, and visible light communications.

BARTHÉLEMY CAGNEAU received the Ph.D. degree from the Institute of Intelligent Systems and Robotics (ISIR), Sorbonne University, in 2008. He became an Associate Professor with the Laboratoire d'Ingénierie des Systèmes de Versailles (LISV), University of Versailles, in 2009. His research interest includes sensors and interactions, especially in the field of micro-robotics.